COMBINING HIGHER ORDER REFLECTIONS WITH DIFFRACTIONS WITHOUT EXPLOSION OF COMPUTATION TIME: THE SOUND PARTICLE RADIOSITY METHOD

Alexander Pohl,
HafenCity University Hamburg
Hamburg, Germany
alexander.pohl@hcu-hamburg.de

Uwe M. Stephenson,
HafenCity University Hamburg
Hamburg, Germany
post@umstephenson.de

ABSTRACT

The simulation of sound propagation in large rooms and urban environments is mainly performed by geometric simulation methods like ray tracing or the Sound Particle Simulation Method (SPSM). Hence, a severe deficiency is that wave effects are not included, especially if screening or diffraction effects are important. A method to introduce diffraction is the Uncertainty relation Based Diffraction (UBD) model, which has been successfully evaluated recently. To find close edges as sources of diffraction, a subdivision of the room into convex subspaces is performed by virtual walls. However, this causes a recursive split-up of Sound Particles (SPs) at each diffraction event. This effect should be compensated by a re-unification of SPs. Therefore, the Sound Particle Radiosity (SPR) has been found that combines the SPSM with an advantage of the radiosity method: the re-unification of sound energy that uses a discretization of the surface into small patches. Now, SPR has been extended to $3D$ for the first time. To increase the available memory and to decrease the computation time, a parallelization has been implemented for the first time. First results indicate that the discretization of the virtual walls into patches yields additional but tolerable errors in the simulation of diffraction. However, even in $2D$, SPR requires a huge memory. To solve this problem in $3D$ remains a great challenge, even more for more complex rooms. Also a method for a convex subdivision to 3D still has to be found.

1. INTRODUCTION

In room as well as in urban acoustics, where the objects are large compared with wavelengths, geometric-energetic simulation methods are applied, like the image source method [1, 2], the SPSM[3], ray tracing [4, 5], or beam tracing[6]. Today, most beam tracing methods assume pyramidal beams[7, 8]. Naturally, all these neglect wave effects. Nevertheless, in the case of SPs, scattering effects are simulated, but diffraction effects are still hardly simulated in a general way. This is a severe deficiency, especially in very jagged rooms with many obstacles as in urban environments, where sound often reaches receivers solely by diffraction. It is important for auralization purposes, too. There are approaches that add first order diffractions based on the rough approximation of the detour law[9] or more accurate wave theoretical approaches[10]. For small reflection orders, it is efficient to combine beam tracing with diffraction[11]. For high reflection orders, even beam tracing becomes inefficient and the SPSM becomes more efficient - especially if a high number of receivers is used[3]. But even with the SPSM, the number of SPs and, hence, the computation time, explodes due to the necessary recursive split-up of SPs. Avoiding the split-up is possible but finally less effective[12]. Thus, a re-unification of SPs is needed. Stephenson proposed[13] that the acoustic radiosity method[14, 15], as known from computer graphics[6], includes such a reunification effect but is restricted to diffuse reflections. Consequently, the SPSM and the radiosity method are combined to the SPR[13, 16] in order to achieve a method that is cable an arbitrary order of specular reflections, scattering and diffraction without an explosion of the computation time. Meanwhile, the UBD diffraction method[12] has been generalized, thoroughly evaluated and combined with the SPR[17].

However, this paper is focused on the algorithmic problems. It is organized as follows: In Sec. 2, the main features of the SPSM are described, whereas the handling of scattering and diffraction is briefly described. Sec. 3 describes the convex subdivision procedure, which is the base for an effective simulation of diffraction. Sec. 4 describes the SPR before Sec. 5, 6 and 7 describe an estimation the SPR efficiency, a method of parallelization and the accuracy of the sound intensities that are computed with the SPR one after another.

2. SOUND PARTICLE SIMULATION METHOD

The SPSM is a typical Monte Carlo method, i.e., the idea is to emit a large number of SPs and to trace them iteratively over a number of reflections. To find the next reflection point, each time a number of walls has to be checked for intersection. Furthermore, the point of intersection on the intersected wall has to be determined. Usually, the termination criterion is related to a maximum number of reflections or the desired length (time range) of the echogram. The number of emitted SPs depends on the desired accuracy (e.g., the uncertainty in the computed sound levels) or the spatial resolution of the room surface.

2.1. Simulation of Multiple Frequency Band Simultaneously

In general, SP propagation paths are strongly dependent on the frequency, such that they are computed for each frequency band independently. In the SPSM, all bands are computed simultaneously. Therefore, SPs are carriers of multiple energies instead of carriers of a single sound energy. Thus, the frequency dependent effects like scattering, diffraction, absorption and air attenuation are only allowed to modify the carried energy, but not the actual sound propagation path.

2.2. Emission of Sound Particles

An equal distribution is simple to realize in $2D$, whereas in $3D$ the unit sphere has to be subdivided into (at least approximately) equally sized regions. A good approximation can be found, e.g., by the EQ Sphere method[18] (see Fig. 1(a)).

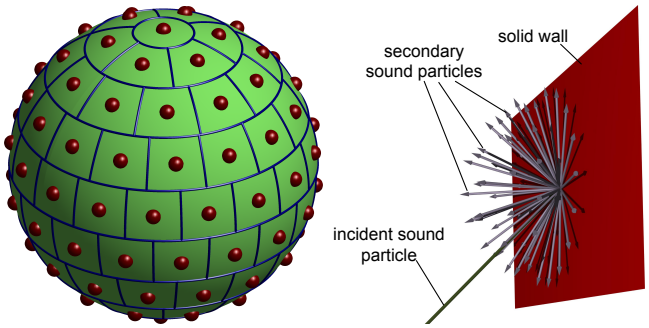

(a) *primary* (b) *secondary*

Figure 1: *Emission of SPs into about equal solid angle ranges without randomization.*

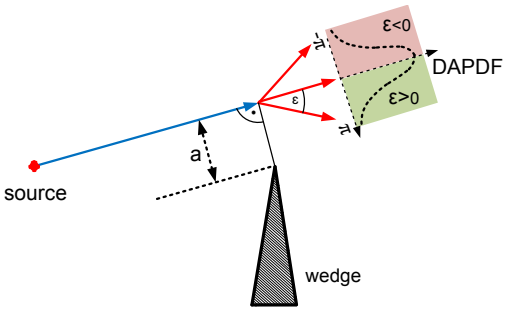

Figure 2: *Diffraction of a SP passing by a single wedge in a distance a by an angle of ε (after Stephenson [12]).*

2.3. Wall Reflection

In case of ideally smooth surfaces, the sound energy is reflected specularly (angle of incidence = angle of reflection). Then, the energy of the SP is reduced by $(1-\alpha)$, where α is the absorption coefficient. In general, α is frequency dependent and, thus, the energies that are carried by the SP have to be modified for each frequency band independently.

2.3.1. Scattering

In case of a rough surface, the ratio of the non-geometrically reflected energy and the total reflected energy is defined as a frequency dependent scattering coefficient σ[19]. To handle scattering in the SPSM, i.e., to define a simple angular characteristic for partially scattering surfaces, commonly used methods[20] interpolate between the geometric reflected energy and the scattered energy distribution according to Lambert's law:

$$\text{in 2D: } \frac{dp}{d\vartheta} = \frac{cos\,(\vartheta)}{2} \text{ and } \quad \text{in 3D: } \frac{dp}{d\Omega} = \frac{cos\,(\vartheta)}{\pi}, \qquad (1)$$

where p is the angular probability density, ϑ the polar and Ω the solid angle, respectively.

In order to avoid a split-up of SPs, these angular probability density functions have been used to compute the direction of the reflected SP. In order to achieve a higher spatial resolution and to keep the sound propagation paths independent of the frequency, a number of S secondary SPs are emitted in equally sized regions (see Fig. 1(b)). The same algorithm as in Sec. 2.2 is used to compute these regions. Each of this SPs carries energies according to an integral over a respective part of the angular probability density function.

2.3.2. Diffraction

In order to introduce edge diffraction into the SPSM, Stephenson proposes to use a diffraction model, which is based on the uncertainty relation[12]. The basic assumptions are: a) edges (for simplification only inner edges) are the main objects where diffraction occurs, b) the SP deflection obeys the uncertainty relation and c) the whole model remains an energetic one. The result is that SPs are diffracted the stronger, the closer (local uncertainty) they pass by an edge (see Fig. 2).

Their deflection is described by a so called Diffraction Angle Probability Density Function (DAPDF), which is derived from the Fraunhofer diffraction at a slit. This UBD diffraction model has been investigated and confirmed in detail during the last years in $2D$, whereas also some approaches exist[17] for the $3D$ case.

This diffraction module is called whenever a virtual wall (see Sec. 3) is intersected by a SP, which indicates one or several close edges. In practice, S secondary SPs that carry energies according to an integral of the DAPDF over the corresponding angle range are emitted. In terms of the algorithm, one difference between scattering and diffraction is that SPs are reflected in the case of scattering, whereas they are transmitted through the virtual wall in the case of diffraction (see Fig. 1(b)). Furthermore, the DAPDF is used instead of Lambert's angular probability density functions.

2.4. Detection of Sound Particles

Ideally thin rays never intersect with point-like receivers. So, small detectors around the receivers are created. In contrast to classical ray tracing, the SPSM takes the distance that a SP travels within this detector into account[17]. Thus, the detectors may have any shape. With rectangular detectors, a dense grid of detectors can be established to simulate an immission area[3]. Maps of different room acoustical parameters can be computed on such a grid. These objective quantities are aimed at and analysed here.

3. CONVEX SUB-DIVISION

Most geometrical acoustic simulation methods use a spatial subdivision technique to decrease the computational effort. In the SPSM, a sub-division into convex subspaces is used, which are interconnected by virtual, i.e., acoustically transparent, walls. The main advantages of this approach are that a) the computation time can be reduced by using only convex polyhedra and b) the virtual walls can be used to detect SPs that have to be diffracted[21].

The spatial data structure in $2D$ is given by a **closed** polygon that delimits the sound propagation area. This polygon is constructed from a set of vertices. As the $2D$ scene is interpreted as a cross-section of the $3D$ space, the vertices that protrude into the sound propagation space are called *inner edges*. Although diffraction occurs on all edges, only inner edges are sources of diffraction in the present paper. Thus, these inner edges have to be the starting point for a convex sub-division (see Fig. 3(a)).

Bisecting lines can be defined at the centre direction of each inner edge (see Fig. 3(a)). In order to avoid additional vertices

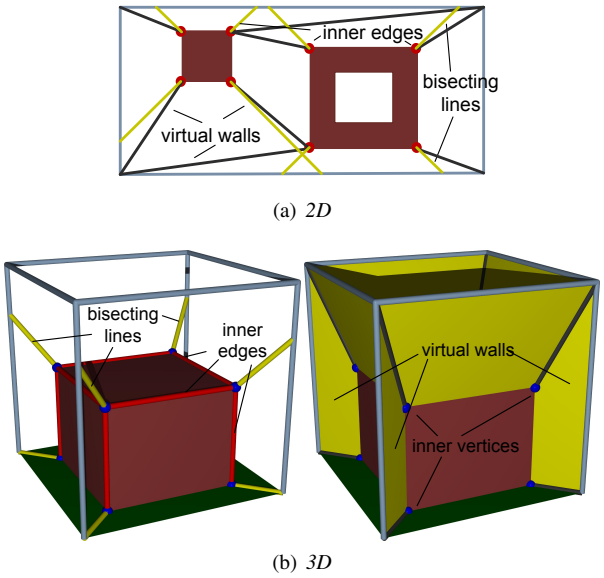

(a) *2D*

(b) *3D*

Figure 3: *Convex Sub-Division by virtual walls.*

(that would increase the complexity again), these bisecting lines are shifted to the closest vertex of the intersected wall. The resulting bisecting lines act as virtual walls. The polygon is divided into two independent sub-spaces at the virtual wall and the algorithm is repeated until no inner edges remain. This algorithm has been implemented and investigated in detail[21]. The result is that the computation time of the SPSM is almost independent of the number of vertices and only depends on a shape factor that describes the ratio between virtual walls and real walls[21].

In $3D$, the spatial data structure is given by a closed polyhedron that is defined by a set of polygons. Therefore, both inner edges and *inner vertices* can be identified (see Fig. 3(b)). Bisecting lines can be defined on each inner vertex and are shifted to the closest vertex of the intersected wall. Virtual walls can be inserted using these constructed lines, but some crucial questions remain open. Here, the result is a set of convex polyhedra that are connect by virtual walls. As this algorithm is not fully implemented in $3D$ yet, both a manual sub-division as well as an automatic sub-division into tetrahedra[22] are used preliminarily. Again, the computation time is dependent on a similar shape factor, describing the ratio of the virtual wall surface and the real surface.

4. SOUND PARTICLE RADIOSITY METHOD

Any recursive split-up of SPs causes an exponential increase of their number and, thus, the computation time. This can only be compensated by a reunification of the SPs. The idea of the radiosity method is to consider a radiation exchange between pairs of small patches of the room surface ending up in solving (directly or iteratively) just a linear equation system[15].

Meanwhile, the radiosity method has been applied and improved in room acoustics. It is either combined with beam tracing to compute the late (diffuse) reflections in a hybrid method[14] or appropriate discretizations without the extension to specular reflections are investigated[23]. Another hybrid method combines the radiosity method with the image source method to allow specular reflections of first order[24]. Furthermore, a generalization of the energy exchange in the radiosity method to specular reflections is presented[25]. However, this method extends the radiosity method by specular reflections on the contrary to an aspired equal weighting of specular and diffuse reflections of the SPR. In order to introduce reunification into the SPSM, Stephenson used the feature of the radiosity method that the number of sound propagation paths, i.e., the number of energy exchange factors, is finite[13]. In the radiosity method, this is achieved by neglecting the history of the sound energy. Stephenson interpreted that as reunification of sound energy on a patch. However, this is the reason that only totally diffuse reflections are possible - the drawback of the radiosity method. In order to allow a generalization to specular reflections, the sound energy is reunified on sound paths **between pairs of patches** rather than on single patches[17] in case of the SPR. Thus, the angle of incidence is not lost anymore. For Stephenson, this is a discretization of both the surface (radiosity method) and the directional space (SPSM)[13]. As a result, the SPR allows the simulation of specular reflections, scattering and even diffraction without an explosion of the computation time.

4.1. Discretization

Three parameters of a SP have to be discretized (see Fig. 4).

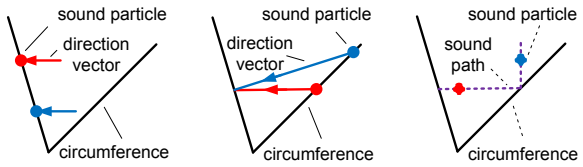

(a) *target point* (b) *emission point (direction of incidence)* (c) *impact time*

Figure 4: *Three parameters describe the SP propagation path.*

To discretize the first two parameters, the circumference of the room is divided into small patches. If SPs intersect with a patch, their intersection points are shifted to the centre of the patch. In addition, the time of incidence on a patch is discretized in time intervals Δt, whose respective traveling distance $c \cdot \Delta t$ is chosen to equal the length of a patch. As SPs that travel less than a time interval might cause infinite loops, these travelled distance are increased to one time interval. As a result, a discretized SP propagation path is completely described by three numbers. A SP only carries energy (or a group of energies for different frequency bands).

4.2. Sound Particle Logistics

In this method, the reunification of SPs happens when they intersect with the room surface. This is plausible, because this is the time when they change their direction or split-up. To allow reunification (in contrast to the SPSM), the SPs have to be traced quasi simultaneously. The problem is: From an algorithmical point of view, this is not possible exactly. Before SPs are traced further from their intermediate position on a patch, they must *wait*, until all *older* SPs on the way have reached this position. In other words, all SPs have to travel a certain distance, before the first SP is allowed to travel further. This processing order can only be

achieved by a completely new frame algorithm. This is performed by a Reunification Matrix (RUM).

4.3. Reunification Matrix (RUM)

The RUM temporary stores SPs and extracts them when needed. It is a multi-dimensional storage of energy, where the parameters of the SPs (the number of the starting patch, the number of the end patch and the number of the impact time interval) are encoded in the position of the energy (see Fig. 5)[16].

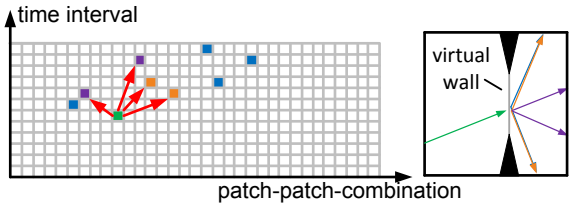

Figure 5: *Example for the SPR process in Reunification Matrix (RUM). To achieve a $2D$-depiction, the number of* ***combinations of the starting point and the end point*** *is shown as the $x-axis$ and the number of the time interval is shown on the $y-axis$.*

Initially, the RUM elements that describe the emission from the sound source are filled with energy (normalized to the sum of 1). Later, always the *oldest*, i.e., least far travelled SP energy (*green element*), is taken out of the RUM. The sound propagation path is reconstructed by the position of the energy. This particle is processed by applying the laws of reflection, diffraction and scattering known from the SPSM. After each step, the SP energy is stored in the RUM at the place corresponding to the intersected patch, the former intersected patch and the time interval of incidence (*red arrows*). Whenever energy is to store in an already occupied element (*orange elements*). Thus, SPs are reunified.

This procedure is repeated, until all energies are transported to the uppermost RUM elements according to the maximum travelling time.

4.4. Definition of Patches

In $2D$, the patches are equally sized line segments of length l_P. In order to have a discretization parameter that is independent of the room size, a relative parameter f_P is introduced

$$f_P = \frac{l_P}{\bar{l}}, \tag{2}$$

where $\bar{l}$ is the mean free patch length of the room. However, in $3D$, a surface instead of a line has to be discretized into patches. One attempt is to perform a triangulation of the wall into equally sized triangles by a refined Delaunay triangulation[26] (see Fig. 6(a)). The drawback is that identifying single triangles and computing their patch number is time consuming.

A huge simplification and more efficient is to place a rectangular grid on the surface (see Fig. 6(b)). Only the determination of the patch centres of patches that contain the wall boundary is demanding. The parameter f_P describes the average patch length.

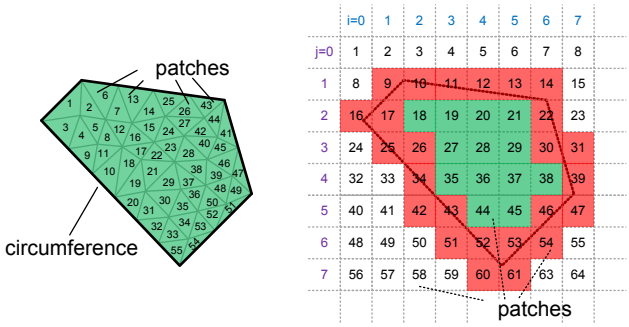

(a) *Delaunay triangulation (after [26])* (b) *regular grid*

Figure 6: *Different techniques defining patches on a surface.*

5. EFFICIENCY OF THE SOUND PARTICLE RADIOSITY ALGORITHM

To determine the speed-up of the SPR relative to the SPSM, two contrary conditions have to be taken into account. On the one hand, the storage of SPs in the RUM causes additional computational effort, whereas, on the other hand, the reunification of SPs reduces the computational effort. Thus, the reunification rate is the main parameter describing the efficiency of the SPR. Furthermore, the computation time of the SPR is investigated to determine the computational effort of reunification.

5.1. Reunification Rate

First, the number of occupied elements $N_{RUM}\,(o)$ after a reflection order o is determined. In this context, reflection order means that each SP is reflected (including scattering or diffraction) o times.

On average, every SP is split-up into $1+S$ secondary SPs when they intersect with a wall. So, the number of occupied matrix elements reads **without reunification**

$$N_{RUM}\,(o) = N \cdot (1+S)^o\,, \tag{3}$$

where N is the number of emitted SPs. With reunification[16], the number of occupied matrix elements is decreased. A recursive formulation reads

$$\begin{aligned} N_{RUM}\,(o+1) &= N_{RUM}\,(o) \cdot q^{N_{RUM}(o)} \\ &+ S \cdot \frac{1-q^{N_{RUM}(o)}}{1-q} \\ N_{RUM}\,(o=0) &= N \text{ with } q = 1 - \frac{S+1}{K_{RUM}}, \end{aligned} \tag{4}$$

where K_{RUM} is the available number of elements in the RUM.

A comparison is given in Fig. 7 for different S.

Without reunification, the number of SPs increases exponentially with the number of computed reflections o. With reunification, the number of occupied matrix elements and, thus, the number of simultaneously existing SPs, is reduced significantly. $N_{RUM}\,(o) = K_{RUM}$ acts as the upper limit of the occupied matrix elements and, hence, SPs.

The size of the RUM is proportional to the product of a) the number of starting patches, b) the (same) number of end patches

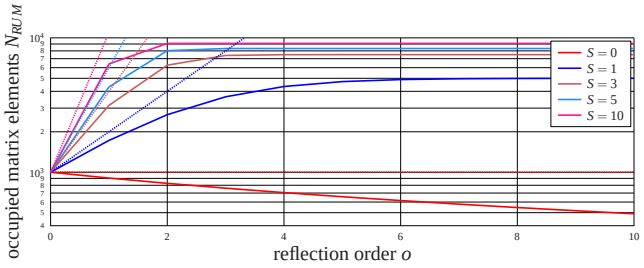

Figure 7: *Number of occupied elements $N_{RUM}\,(o)$ as a function of the reflection order o, with different split-up values S. The estimated number of occupied elements with reunification (solid, SPR) is compared to the case without reunification (dotted, SPSM)*

and c) the number of time intervals. The number of time intervals is reduced by recycling the RUM after a maximum free path length (room diagonal) has been travelled. For a quadratic (cubical) room, the number of available matrix elements turns out to be

$$K_{RUM,2D} \approx 47 \cdot \frac{1}{f_P^3} \text{ and } K_{RUM,3D} \approx 474 \cdot \frac{1}{f_P^5} \qquad (5)$$

In case of a more complex scene, this size increases only linearly with the number of convex sub-spaces (another advantage of the sub-division). A modern computer with $16GB$ RAM allows maximum discretization factors of $f_P \approx \frac{1}{450}$ in $2D$ or $f_P \approx \frac{1}{25}$ in $3D$.

5.2. Computation Time

The computation times have been measured by a simulation of a two dimensional, rectangular room with $N = 1000$ primary SPs and a split-up of $S = 25$. The computation times of the SPR and the SPSM are compared in Fig. 8.

Figure 8: *Computation times of Sound Particle Radiosity (SPR).*

As expected, the computation time of the SPSM increases exponentially with the reflection order (note the logarithmic $y - scale$). Compared to this, the computation time of the SPR is reduced. With this set-up, both computation times are equal at approximately $o_{Max} = 4$. For higher reflection orders, the SPR is faster than the SPSM, but the SPSM is still faster for lower reflection orders. For only one reflection, the SPSM computes less than a second, whereas SPR already has a computation time of approximately one minute. The reason for this behaviour is the additional computational effort to access the RUM.

6. PARALLELIZATION

Besides the reduction of computation time, another main purpose of parallelization is to add additional memory by using computer clusters[27]. For efficiency, the idea is to assign a part of the RUM to every computer. A simple approach is to assign all RUM elements that describe the sound propagation paths within the same convex sub-space to the same computer. The bottleneck of these computer clusters is the communication between distributed computers. To reduce this, a good decomposition of the RUM is needed. In the RUM, each *column* (see Fig. 5) represents a sound propagation path, i.e., a patch-patch combination. The nodes in the graphs (see Fig. 9) depict RUM elements and the arrows sequences of sound propagation paths, i.e., communications between matrix elements. The boundary between RUM elements of different computers (in reality: maybe of different sub-spaces) is indicated by a *red* edge (see Fig. 9). Every transfer between different (sub-)RUMs is called edgecut. The number of these edgecuts indicates the amount of communication overhead (remote calls), which has to be reduced. For an example of eight *columns*, two different decompositions are shown in Fig. 9.

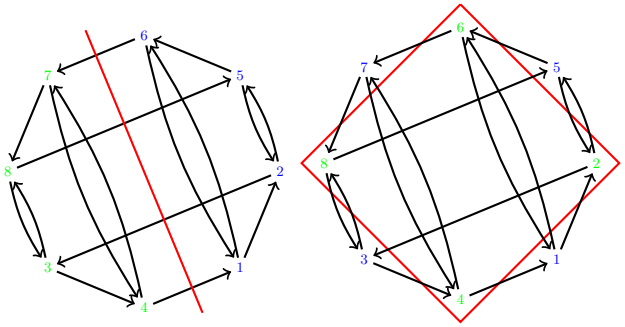

(a) 4 *edgecuts* (b) 16 *edgecuts*

Figure 9: *Two decompositions of eight matrix elements in a graph model.*

A good decomposition is one that minimizes the remote calls. In our experiments, a standard toolbox has been used[27]. For further experiments, however, it is advisable to exploit geometrical information, i.e., the transfer probabilities between pairs of patches. They are increased for patch-patch-combinations within parallel and specularly reflecting walls (causing flutter echoes) or reduced in case of patch-patch-combinations that are distributed among distant sub-spaces.

7. ACCURACY OF SOME COMPUTED ROOM ACOUSTICAL PARAMETERS

Due to the discretization of the sound propagation paths, numerical errors are produced - especially within the simulation of diffraction. In order to determine the accuray of the SPR method, three parameters are computed: a) the relative error of the total sound intensity, b) the relative error of a short time intervall of an echogram and c) the relative error of the reverberation time. The result of a SPSM simulation, i.e., without discretization, serves as reference. All errors are strongly dependent on the discretization parameter f_P.

7.1. Influence of the Patch Size in 2D

In a first attempt, simulations have been performed without scattering or diffraction to focus on the numerical error due to the discretization.

The geometrical scene is defined by a rectangular room with walls of length $a = 10m$ and 81 receivers with a diameter of $r_D = 1m$. The maximum simulation time, and thus the maximum length of the echogram, is restricted to $T_{Max} = 0.1s$ to focus on single reflections. The echogram is split up into 1000 time intervals of $\Delta t = 0.1ms$. The absorption degrees are set to $\alpha = 0.5$ and scattering is disabled ($\sigma = 0.0$, $S = 0$) on all four walls. The echogram that is simulated with the SPR converges to the echogram that is simulated with SPSM for decreasing discretization parameters f_P. Only slight differences occur for $f_P = 1/100$, but strong deviation occur for $f_P = 1/20$.

For all receivers, the reverberation time and the total sound intensity are computed with the SPR are their errors are defined relative to the results of the SPSM. Both values are below 2% for $f_P < 1/100$ and increase only up to 20% for $f_P = 1/10$. The reason is that small variations of the sound propagation path only slightly affect both the reverberation time and the total intensity. However, the average error in a single time slot is 300% for $f_P = 1/20$ and 50% for $f_P = 1/200$. Here, slight time shifts cause a detection in adjacent time intervals. (A graph is omitted, because the echograms are similar to Fig. 10).

7.2. Influence of the Patch Size in 3D

The same experiment has recently been performed for a cubical room. The dimensions are adjusted to $a = 11.78m$ and $r_D = 1.178m$ in order to have the same mean free path length as in the former experiment. An example of one of the 729 receivers (filling the whole cube) is shown in Fig. 10. The result is similar to the

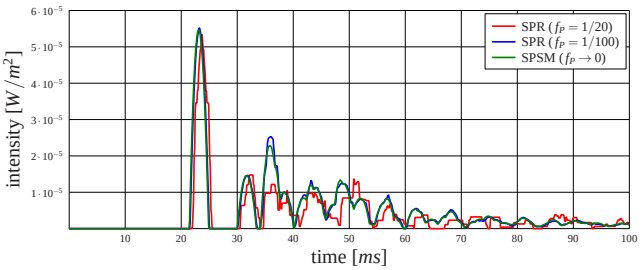

Figure 10: *Echograms of different discretizations in 3D.*

$2D$ result, which is confirmed by the numerical results of the error in reverberation time and total sound intensity. Quantitatively, the average error in a time interval in increased by a factor of 2 compared with the $2D$ result.

7.3. Influence of the Discretization on the Simulation of Diffraction

In case of diffraction, the spatial behaviour of the numerical errors is more important than its time behaviour. Due to the functional principle of SPR, all SPs are discretized by shifting their intersection points to the patch centres before they are diffracted or detected. Former investigations revealed that at least one SP has to be diffracted in the region of $d = 0.1\lambda$ above the wedge. This region is in the range of $0.002m(16.000Hz) < d < 1.092m(31.5Hz)$ (Here: $6.8cm$ at $500Hz$). The simulations have been performed in a $2D$ rectangular room with a width of $a = 20m$ in each dimension. A single wedge with a height of $a/2 = 10m$ is placed on the centre of the floor. The source is placed in the centre of the subspace on the left-hand side of the wedge (see Fig. 11). No specified receiver position is needed, because a sound intensity map is computed for a whole receiver grid. These receivers are placed is a distance of $w_{grid} = 0.1m$ that equals their diameter ($200x200$ receivers). All surfaces (incl. wedge) are fully absorbent ($\alpha = 1.0$) to focus on the effect of diffraction). A sufficient number of $N = 500.000$ primary SPs are emitted and split up into $S = 200$ SPs at each diffraction[17].

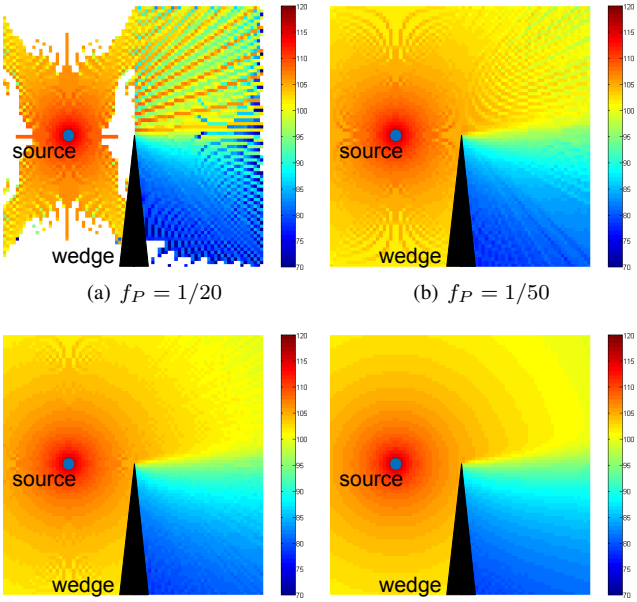

(a) $f_P = 1/20$ (b) $f_P = 1/50$

(c) $f_P = 1/100$ (d) *SPSM* $f_P \to 0$

Figure 11: *Sound intensity levels for different discretizations of a diffraction simulation at $f = 500Hz$ in a quadratic, fully absorbent room.*

Again, the numerical error decreases with decreasing discretization parameters. To describe the influence of the discretization error on diffraction quantitatively, the average over the absolute level difference is investigated for all frequency bands (relative to the respective SPSM) in the shadow zone ($1dB$ at $f = 500Hz$ and $f_P = 1/50$).

The error is shown to be strongly influenced by the ratio of the patch length and the wavelength and only hardly dependent on the absolute patch size. As a result, the patch length has to be adjusted to meet the requirements for the highest frequency simulated. For an accuracy of $1dB$ even at $4kHz$, a discretization parameter of $f_P \leq \frac{1}{250}$ is required.

8. CONCLUSION AND OUTLOOK

Due to the reunification effect, the SPR allows a room acoustical simulation including diffraction or scattering of an arbitrary order without an explosion of the computation time. It has been implemented in $3D$ and on a computer cluster for the first time. The SPR

frame algorithm is identical in $2D$ and $3D$. The spatial discretization of the surface has been performed using quadratic patches for the first time. However, the size of the RUM increases to the power of 5 in $3D$ instead of the power of 3 in $2D$ with the discretization parameter. This huge size is still the main drawback of the SPR, which can be compensated only by part using parallelization.

The concept of the convex sub-division still has to be fully implemented in $3D$. The diffraction module is already analytically defined and tested in $3D$ for simple setups[17] and a combination with the SPR algorithm is in preparation. However, the main challenge is to find a method to reduce the required memory.

9. REFERENCES

[1] J. B. Allen and D. A. Berkley, "Image method for efficiently simulating small-room acoustics," *The Journal of the Acoustical Society of America*, vol. 65, no. 4, pp. 943–950, 1979.

[2] J. Borish, "Extension of the image model to arbitrary polyhedra," *The Journal of the Acoustical Society of America*, vol. 75, no. 6, pp. 1827–1836, 1984.

[3] Uwe M. Stephenson, "Comparison of the mirror image sourc emethod and the sound particle simulation method," *Applied Acoustics*, vol. 29, no. 1, pp. 35–72, 1990.

[4] A. Krokstad, S. Strom, and S. SÃ¸rsdal, "Calculating the acoustical room response by the use of a ray tracing technique," *Journal of Sound and Vibration*, vol. 8, no. 1, pp. 118 – 125, 1968.

[5] Michael Vorländer, "Simulation of transient and steady-state sound propagation in rooms using a new combined ray-tracing/image-source algorithm," *The Journal of the Acoustical Society of America*, vol. 86, no. 7, pp. 172–178, 1989.

[6] Andrew S. Glassner, Ed., *An introduction to ray tracing*, Academic Press Ltd., London, UK, 1989.

[7] A. Farina, "RAMSETE - a new Pyramid Tracer for medium and large scale acoustic problems," in *Proceedings of the Euronoise*, Lyon, France, 1995.

[8] Thomas Funkhouser, Ingrid Carlbom, Gary Elko, Gopal Pingali, Mohan Sondhi, and Jim West, "A beam tracing approach to acoustic modeling for interactive virtual environments," in *Proceedings of the 25th Annual Conference on Computer Graphics and Interactive Techniques*, New York, NY, USA, 1998, SIGGRAPH '98, pp. 21–32, ACM.

[9] Z. Maekawa, "Noise reduction by screens," *Applied Acoustics*, vol. 1, no. 3, pp. 157–173, 1968.

[10] U. P. Svensson, R. I. Fred, and J. Vanderkooy, "An analytic secondary source model of edge diffraction impulse responses," *The Journal of the Acoustical Society of America*, vol. 106, pp. 2331–2344, 1999.

[11] Nicolas Tsingos, Thomas Funkhouser, Addy Ngan, and Ingrid Carlbom, "Modeling acoustics in virtual environments using the uniform theory of diffraction," in *Proceedings of the 28th annual conference on Computer graphics and interactive techniques*, New York, NY, USA, 2001, SIGGRAPH '01, pp. 545–552, ACM.

[12] Uwe M. Stephenson, "An energetic approach for the simulation of diffraction within ray tracing based on the uncertainty relation," *Acta Acustica united with Acustica*, vol. 96, pp. 516–535, 2010.

[13] Uwe M. Stephenson, "Quantized pyramidal beamtracing or a sound-particle-radiosity- algorithm? - new solutions for the simulation of diffraction without explosion of computation time," in *Proceedings of the Research Symposium on Acoustic Characteristics of Surfaces*, Salford, United Kingdom, 2003.

[14] T. Lewers, "A combined beam tracing and radiatn exchange computer model of room acoustics," *Applied Acoustics*, vol. 38, no. 2–4, pp. 161–178, 1993.

[15] H. Kuttruff, "A simple iteration scheme for the computation of decay constants in enclosures with diffusely reflecting boundaries," *The Journal of the Acoustical Society of America*, vol. 98, no. 1, pp. 288–293, 1995.

[16] Alexander Pohl and Uwe M. Stephenson, "A combination of the sound particle simulation method and the radiosity method," *The Journal of Building Acoustics*, vol. 18, no. 1, pp. 97–122, 2011.

[17] Alexander Pohl, *Simulation of Diffraction Based on the Uncertainty Relation – An Efficient Simulation Method Combining Higher Order Diffractions and Reflections*, Ph.D. thesis, HafenCity University Hamburg, 2014.

[18] Paul Leopardi, *Distributing points on the sphere: Partitions, separation, quadrature and energy*, Ph.D. thesis, The University of New South Wales, 2007.

[19] "ISO 17497 Part 1: Measurement of random-incidence scattering coefficient in a reverberation room," 2004.

[20] Dirk Schröder and Alexander Pohl, "Modeling (non-) uniform scattering distributions in geometrical acoustics," in *Proceedings of International Congress on Acoustics*, Montreal, Canada, 2013.

[21] Alexander Pohl and Uwe M. Stephenson, "Efficient simulation of sound propagation including multiple diffractions in urban geometries by convex sub-division," in *Proceedings of Internoise*, Lisbon, Portugal, 2010.

[22] Hang Si, *Three Dimensional Boundary Conforming Delaunay Mesh Generation*, Ph.D. thesis, Technische Universität Berlin, 2008.

[23] Eva-Marie Nosal, Murray Hodgson, and Ian Ashdown, "Improved algorithms and methods for room sound-field prediction by acoustical radiosity in arbitrary polyhedral rooms," *The Journal of the Acoustical Society of America*, vol. 116, no. 2, pp. 970–980, 2004.

[24] N. Korany, J. Blauert, and O. Abdel Alim, "Acoustic simulation of rooms with boundaries of partially specular reflectivity," *Applied Acoustics*, vol. 62, no. 7, pp. 875 – 887, 2001.

[25] Samuel Siltanen, Tapio Lokki, Sami Kiminki, and Lauri Savioja, "The room acoustic rendering equation," *The Journal of the Acoustical Society of America*, vol. 122, no. 3, pp. 1624—1645, 2007.

[26] Jonathan Richard Shewchuk, "Robust Adaptive Floating-Point Geometric Predicates," in *Proceedings of the Twelfth Annual Symposium on Computational Geometry*. 1996, pp. 141–150, Association for Computing Machinery.

[27] Alexander Pohl, Jan Winkelmann, and Uwe M. Stephenson, "Parallel sound particle radiosity: Reunification of diffracted and scattered sound particles on parallel computers," in *Proceedings of DAGA*, Meran, Italy, 2013.